Journal of Marine Science and Technology

Volume 20 | Issue 3 Article 4

USING MERCURY INTRUSION POROSIMETRY TO STUDY THE INTERFACIAL PROPERTIES OF CEMENT-BASED MATERIALS

Shih-Wei Cho
Department of Architecture, China University of Science and Technology, Taipei City, Taiwan, R.O.C.,
swcho@cc.cust.edu.tw

USING MERCURY INTRUSION POROSIMETRY TO STUDY THE INTERFACIAL PROPERTIES OF CEMENT-BASED MATERIALS

Acknowledgements

The financial support of National Science Council in ROC under the grants NSC 95-2211-E-157-008 is gratefully appreciated.

USING MERCURY INTRUSION POROSIMETRY TO STUDY THE INTERFACIAL PROPERTIES OF CEMENT-BASED MATERIALS

Shih-Wei Cho

Key words: interface transition zone, mercury intrusion porosimetry, durability, cement-based material.

ABSTRACT

Cement-based material is a typical porous composite material. Pore structures and interfacial properties of cement-based materials are influenced properties of ion transport behavior and durability. This study determines pore structure by employing mercury intrusion porosimetry (MIP), with mortar specimens manufactured with three different water-cement (w/c) ratios and five volume proportions of fine aggregate to investigate interfacial properties. The experimental results show that total mercury intrusion decreases with an increase in sand volume proportion when comparing the same w/c ratio. The calculated mercury intrusion of interfacial transition zone increases with w/c and the volume proportion of fine aggregate.

I. INTRODUCTION

Cement-based materials are multiphase, non-homogeneous composites. Because the volume of hydration products does not equal the total volume of water and cement before setting, and since air bubbles are introduced via tamping, a large number of voids or pores surface inside cement-based materials. Several studies have investigated the pore structure of cement-based materials and classified five types of pores from the macro to nano scale, including entrapped and entrained air pores, capillary pores, and gel pores that exist in cement paste [6]. The sparse region (interface transition zone, ITZ) between paste and aggregate is a type of pore [2, 5]. Especially in capillary pores and ITZ, pores are connected and influence reinforced concrete durability of chloride diffusion [1, 10]. Current assessments of pore properties mainly employ water absorption tests because the test procedures are easy and yield rapid results. Specimens are soaked in water to reach a constant weight, and weight differences between oven conditions reflect the porosity of specimens. However, the pore structures of cement-based materials cannot be found and described using these test results because certain pores with small diameters cannot absorb water rapidly during water absorption tests. Alternatively, mercury intrusion porosimetry (MIP) is another method that can investigate the pore structure, which utilizes high-pressure oil to press mercury into the specimen and measure the mercury intrusion volume at different pressure points to reflect the connective pore structure. Certain studies have implemented this method to analyze the pore structure of cement-based materials. For example, Ramezanianpour employed MIP to study the curing effects of porosity on concrete-incorporating slag, fly ash, or silica fume [9], and O'Farrell *et al*. examined the pore size distribution of waste brick mortar via MIP [7]. This study considered mortar as a cement-based composite, obtaining the connective pore structure of mortar specimens by using an MIP test, and using the results to assess the effects of sand volume in mortar.

II. EXPERIMENTAL PROGRAM

1. Materials and Specimen Preparation

This study defines mortar as a multiphase composite in which the inclusion of fine aggregate is joined into a matrix of paste, which was composed of Type I cement, with water/cement ratios of 0.3, 0.4, and 0.5. Ottawa standard sand (sieve sizes between #16 and #30, fitting the requirements of ASTM C778) was used as fine aggregate. To investigate the pore structure change, this study considered different sand volume proportions (volume of fine aggregate/total mix volume), ranging from 0.1 m^3/m^3 to 0.4 m^3/m^3 in mortar mixtures. The mixture proportions of the mortar are summarized in Table 1. Regarding the mixtures, the first letter indicates w/c ratios A, B, and C, and the number represents the sand volume. Cylindrical specimens ($\psi 2.5 \times 2.5$ cm) were cast and cured in water. At 91 days, all the cylinders were stored in an air-conditioned room (25 ± 2°C and 60 ± 5% RH) for a minimum of 14 days. For A series mixes, the additive of superplasticizer was adjusted to obtain the required workability.

Paper submitted 03/25/11; revised 06/26/11; accepted 09/09/11. *Author for correspondence: Shih-Wei Cho (e-mail: swcho@cc.cust.edu.tw).*
Department of Architecture, China University of Science and Technology, Taipei City, Taiwan, R.O.C.

Table 1. Mix design.

No.	w/c	Cement (kg/m^3)	water (kg/m^3)	Fine aggregate (kg/m^3)	HRWR* (kg/m^3)
A0	0.3	1592	462	-	16
A1	0.3	1429	414	259	14
A2	0.3	1267	367	519	13
A3	0.3	1104	320	778	11
A4	0.3	942	273	1037	9
B0	0.4	1366	546	-	-
B1	0.4	1227	491	259	-
B2	0.4	1087	435	519	-
B3	0.4	948	379	778	-
B4	0.4	808	323	1037	-
C0	0.5	1199	599	-	-
C1	0.5	1077	538	259	-
C2	0.5	954	477	519	-
C3	0.5	832	416	778	-
C4	0.5	710	355	1037	-

*High Range Water Reducer, ASTM C944 Type F.

2. Testing Methods

The pore structure of the specimens was determined via mercury intrusion porosimetry. This measurement was performed with the Micromeritics AutoPore IV. The specimen was placed in a glass tube and filled with a non-wetting liquid (mercury) under vacuum conditions (a pressure of less than 50 μm/Hg). The glass tube with the specimen and mercury was subsequently placed in a high-pressure analysis port. The high-pressure analysis port utilized oil to continue pressing mercury into the specimen, with a pressure ranging from 14.7 psi to 60,000 psi, and the intrusion mercury volume was recorded at each pressure point. Washburn's equation [8] transformed the pressure value into the pore diameter, as expressed in Eq. (1):

$$d_p = \frac{-4 * \sigma^{Hg} * \cos(\theta)}{p * k} \quad (1)$$

where d_p is the pore diameter (μm); σ^{Hg} is the surface tension of mercury (dynes/cm); θ is the contact angle between mercury and the specimen surface; p is the press pressure (psi); and k is the transfer constant (10^{-4} cm/μm × 68947 psi/dynes × cm^{-2}). The maximum pressure of 60,000 psi represents the mercury intruding into pores, down to approximately 3 nm.

III. RESULTS AND DISCUSSION

The mercury intrusion results of the C0 specimen are plotted in Fig. 1. Which displays two lines to show the relationship between mercury intrusion and pore sizes. The solid line represents the cumulative intrusion, reflecting the total connected pore volume of pore sizes larger than a specified radius. The dashed line represents the incremental intrusion at each pore radius and the reflected pore volume at that as well, which indicates that most pore radii of the C0 specimen are distributed between 40 nm to 100 nm.

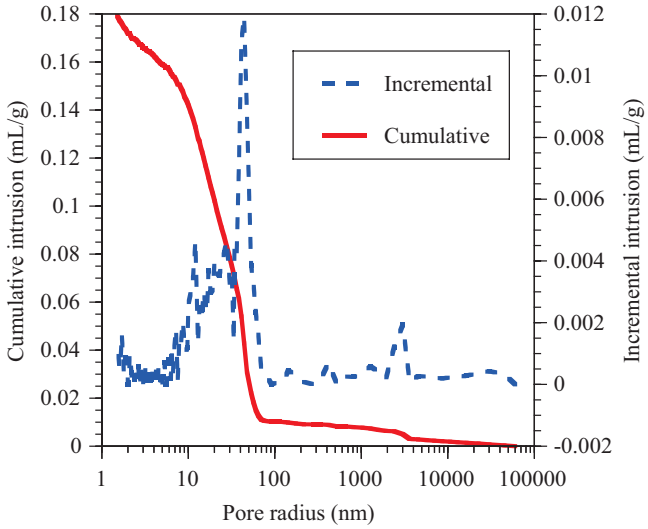

Fig. 1. Variations of mercury intrusion volume for 0.5 w/c paste (Mix C0).

Fig. 2 shows the cumulative intrusion results of the A, B, and C series, and the total mercury intrusion is summarized in Table 2. Fig. 3 shows the relationship between total mercury intrusion and the volume proportion of fine aggregate, which shows that total mercury intrusion increases in conjunction with the w/c ratio. When w/c = 0.3, the total mercury intrusion of specimens with different sand volume proportions are 0.098~0.061 ml/g for the A series; 0.126~0.079 mL/g for the B series (w/c = 0.4); and 0.172~0.111 mL/g for the C series (w/c = 0.5). The total mercury intrusion decreases alongside an increase in sand volume proportion when comparing the same w/c ratio. This reflects the fact that different pore sizes result in different phenomena with the intrusion pole volume of total mercury intrusion. Fig. 4 shows the intrusion pore volume of total mercury intrusion with different pore size ranges, which are divided into 7 parts (>10,000 nm, 10,000-1000 nm, 1000-500 nm, 500-100 nm, 100-50 nm, 50-10 nm, and <10 nm). This shows that volumes of pore sizes smaller than 10 nm increase in conjunction with w/c ratio.

A large number of studies have indicated that the size of capillary pores was 10-10,000 nm, and the thickness of ITZ was approximately 10-500 nm [3, 4, 11]. Fig. 5 shows the relationship between the intrusion volume of pore size in the range of 10-10,000 nm and the volume proportion of fine aggregate. The results share the same trend shown in Fig. 3. However, they cannot classify the pore structure capillary pores and ITZ. This study considered cement paste as a matrix with an inclusion of fine aggregate. The capillary pores exist in cement paste, and ITZ is a sparse layer between the matrix and inclusion. To investigate the pore structure of ITZ, which

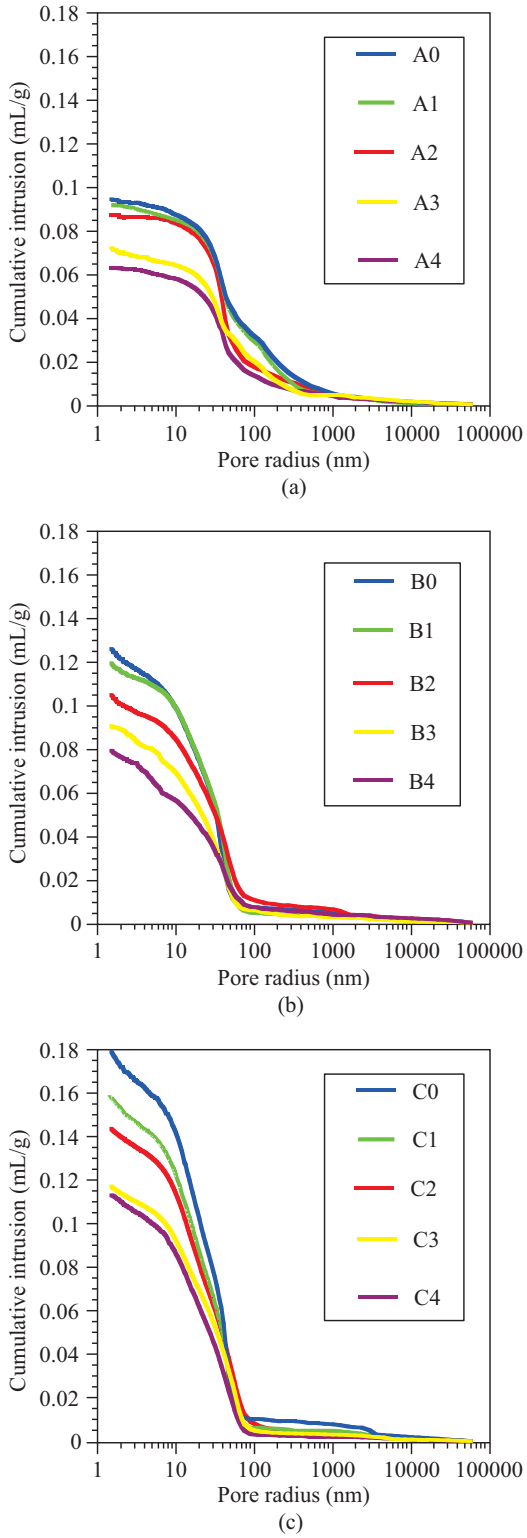

Fig. 2. Variations of cumulative intrusion for mortar with (a) 0.3 w/c, (b) 0.4 w/c, and (c) w/c = 0.5.

is considered a uniform layer around the fine aggregate, and the aggregate with ITZ does not overlap, the pore structure of mortar can be expressed as:

Table 2. Total mercury intrusion of specimens (mL/g).

No.	Specimen 1	Specimen 2	Specimen 3	Average
A0	0.09433	0.09955	0.09959	0.09782
A1	0.09092	0.08790	0.08890	0.08924
A2	0.08157	0.07806	0.07973	0.07979
A3	0.06652	0.07170	0.07311	0.07044
A4	0.06259	0.06003	0.05980	0.06081
B0	0.12593	0.12702	0.12650	0.12648
B1	0.11939	0.10999	0.11450	0.11463
B2	0.10471	0.10214	0.10250	0.10312
B3	0.09263	0.09002	0.09085	0.09117
B4	0.07857	0.07820	0.08104	0.07927
C0	0.17817	0.16985	0.16656	0.17153
C1	0.15808	0.15463	0.16002	0.15758
C2	0.14137	0.14144	0.14037	0.14106
C3	0.12301	0.12768	0.12920	0.12663
C4	0.10591	0.10950	0.11621	0.11054

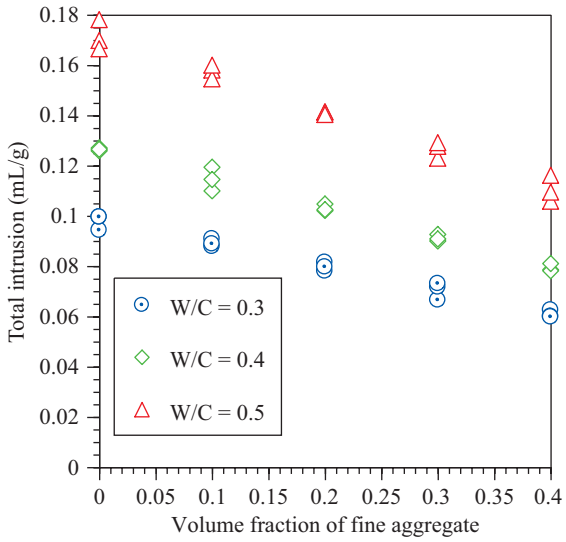

Fig. 3. Total intrusion of specimen *vs*. volume fraction of fine aggregate.

$$P_{total} = P_p(1-V_a) + P_{ITZ} + P_a \quad (2)$$

where P_{total} is the total mercury inclusion (mL/g) of the mortar composite; P_p is the total mercury inclusion (mL/g) of the matrix (cement paste); V_a is the volume proportion of the fine aggregate; P_{ITZ} is the mercury inclusion (mL/g) of ITZ; and P_a is the mercury inclusion of the fine aggregate, and is sufficiently small to be neglected. P_{ITZ} is thereafter calculated in Eq. (3), as follows:

$$P_{ITZ} = P_{total} - P_p(1-V_a) \quad (3)$$

Table 3 shows the calculated value of P_{ITZ}. The relationship between P_{ITZ} and the volume proportion of fine aggregate are

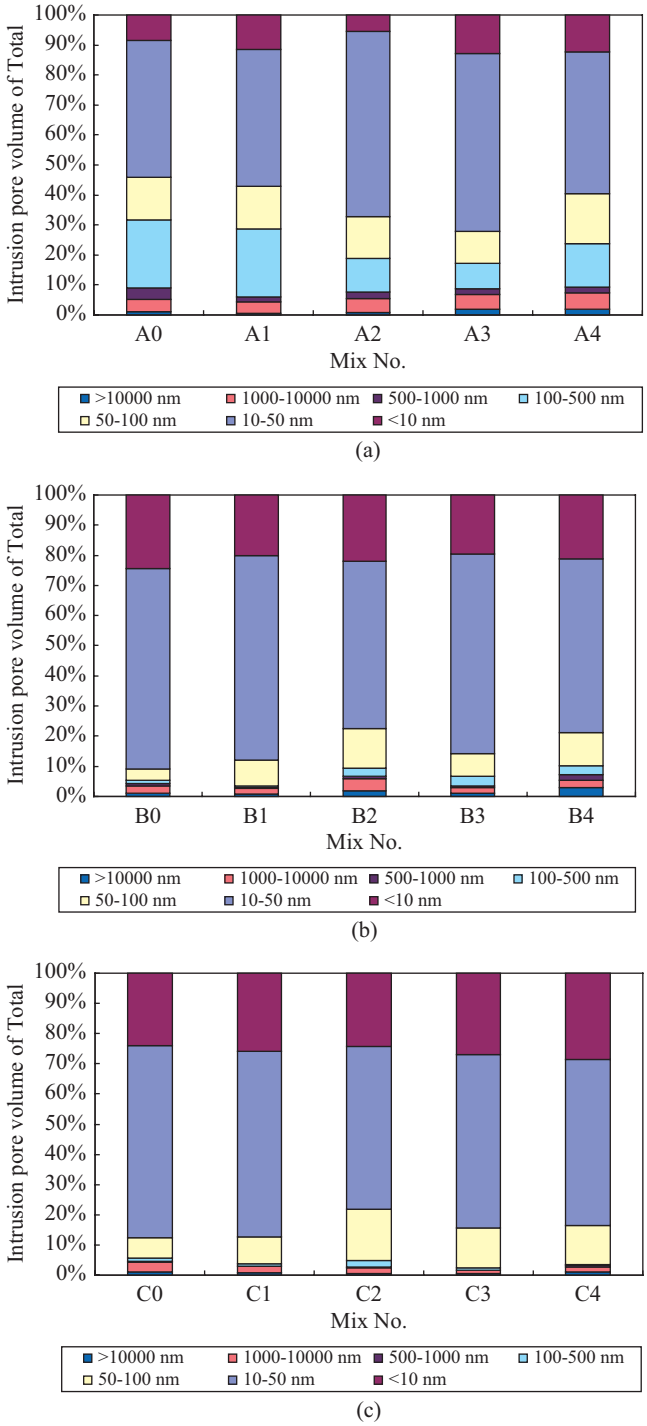

Fig. 4. Intrusion pore volume of total mercury intrusion at different pore size range for mortar with (a) 0.3 w/c, (b) 0.4 w/c, and (c) w/c = 0.5.

shown in Fig. 6. P_{ITZ} increases in conjunction with w/c and the volume proportion of fine aggregate. The difference between 50% of the volume proportion and matrix (volume proportion = 0%) increases alongside w/c, which shows that the weak zone between the paste and aggregate increases in conjunction with w/c.

Table 3. The calculated value of P_{ITZ}.

Mix	P_{ITZ} (mL/g)	Mix	P_{ITZ} (mL/g)	Mix	P_{ITZ} (mL/g)
A0	0.00000	B0	0.00000	C0	0.00000
A1	0.00316	B1	0.00332	C1	0.00663
A2	0.00348	B2	0.00446	C2	0.00727
A3	0.00392	B3	0.00516	C3	0.00999
A4	0.00407	B4	0.00591	C4	0.01106

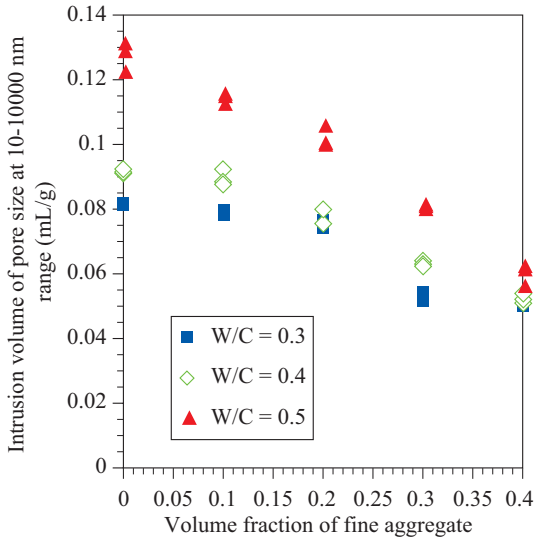

Fig. 5. Intrusion volume of pore size at 10-10000 nm range *vs.* volume fraction of fine aggregate.

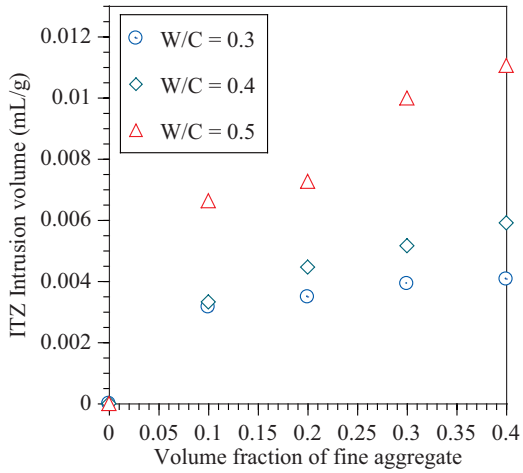

Fig. 6. Intrusion volume of ITZ *vs.* volume fraction of fine aggregate.

IV. CONCLUSION

This study employed the MIP test to examine the connective pore structure of mortar specimens. Future work should clarify the thickness and properties of ITZ. Based on the experimental results, this study presents the following conclusions:

(1) Total mercury intrusion of the specimen increases alongside the w/c ratio. When w/c = 0.3, the total mercury intrusion of specimens with different sand volume are 0.098~0.061 ml/g for the A series; 0.126 ~0.079 mL/g for the B series (w/c = 0.4); and 0.172~0.111 mL/g for the C series (w/c = 0.5).
(2) Total mercury intrusion decreases alongside an increase in sand volume proportion when comparing the same w/c ratio. The intrusion volume of pore size at a range of 10-10,000 nm shares the same trend.
(3) The calculated mercury intrusion of ITZ increases alongside w/c and the volume proportion of fine aggregate, which shows that the weak zone between the paste and aggregate expands with an increase in w/c.

ACKOWLEDGMENTS

The financial support of National Science Council in ROC under the grants NSC 95-2211-E-157-008 is gratefully appreciated.

REFERENCES

1. Brandt, A. M., *Cement-Based Composites: Materials, Mechanical Properties and Performance*, E & FN SPON, London, pp. 116-118 (1995).
2. Carles-Gibergues, D. A., Ballivy, G., and Grandet, J., "Contribution to the formation mechanism of the transition zone between rock-cement paste," *Cement and Concrete Research*, Vol. 23, No. 2, pp. 335-346 (1993).
3. Delagrave, A., Bigas, J. P., Olivier, J. P., Marchand, J., and Pigeon, M., "Influence of the interfacial zone on the chloride diffusivity of mortars," *Advance in Cement Based Materials*, Vol. 5, Nos. 3-4, pp. 86-92 (1997).
4. McCarter, W. J., Emerson, M., and Ezirim, H., "Properties of concrete in the cover zone: developments in monitoring techniques," *Magazine of Concrete Research*, Vol. 47, No. 172, pp. 243-251 (1995).
5. McCarter, W. J., Emerson, M., and Ezirim, H., "Properties of concrete in the cover zone: water penetration, sorptivity and ionic ingress," *Magazine of Concrete Research*, Vol. 48, No. 176, pp. 149-156 (1996).
6. Mindess, S., Young, J. F., and Darwin, D., *Concrete*, Pearson Education, New Jersey, pp. 75-76 (2003).
7. O'Farrell, M., Wild, S., and Sabir, B. B., "Pore size distribution and compressive strength of waste clay brick mortar," *Cement and Concrete Composites*, Vol. 23, No. 1, pp. 81-91 (2001).
8. Paul, A. W., *An Introduction to the Physical Characterization of Materials by Mercury Intrusion Porosimetry with Emphasis on Reduction and Presentation of Experimental Data*, Micromeritics Instrument Corporation, Atlanta, pp. 6-7 (2001).
9. Ramezanianpour, A. A., "Effect of curing on the compressive strength resistance to chloride-ion penetration and porosity of concrete incorporating slag, fly ash or silica fume," C*ement and Concrete Composites*, Vol. 17, No. 2, pp. 125-133 (1995).
10. Yang, C. C. and Cho, S. W., "Approximate migration coefficient of percolated interfacial transition zone by using the accelerated chloride migration test," *Cement and Concrete Research*, Vol. 35, No. 2, pp. 344-350 (2005).
11. Yang, C. C. and Su, J. K., "Approximate migration coefficient of interfacial transition zone and the effect of aggregate content on the migration coefficient of mortar," *Cement and Concrete Research*, Vol. 32, No. 10, pp. 1559-1565 (2002).